Russian Chemical Reviews **76** (5) 463 – 470 (2007) © 2007 Russian Academy of Sciences and Turpion Ltd

DOI 10.1070/RC2007v076n05ABEH003679

Multifunctional nanostructured films

E A Levashov, D V Shtansky

Contents

I. Introduction 463
II. Multicomponent nanostructured films for mechanical engineering 464
III. Multifunctional nanostructured films for medicine 467

Abstract. The state-of-the-art of investigation into multifunctional (multicomponent) nanostructured films used in mechanical engineering and medicine is considered. The bibliography includes 113 references.

I. Introduction

New materials form the basis for the technology of the 21st century, and the industry of nanomaterials is a priority field of development of science and engineering. An important vigorously developing trend in the nanomaterial and nanotechnology sciences is the surface engineering, in particular, the design of multicomponent (multifunctional) nanostructured films (MNF) with a characteristic crystallite size of 1 to 100 nm (Fig. 1).[1]

What makes nanostructured films unique is the high volume fraction and strength of interfaces, the absence of dislocations inside the crystallites, the possibility of changing the ratio of the volume fractions of the crystalline and amorphous phases and the mutual solubility of metal and non-metal components. The presence of a large interfacial area (the volume fraction may reach 50%) in nanostructured films allows one to change their properties either by material and electronic structure modification † or by doping. The strength of the interfaces favours the stability of nanostructured films against deformation. The lack of dislocations inside the crystallites increases the elasticity of these films. These factors altogether allow the production of nanomaterials with improved physicochemical and physicomechanical characteristics, namely, with high hardness ($H > 30$ GPa), elastic recovery ($W_e > 70\%$), strength, thermal stability, and heat and corrosion resistance.

An important feature of the ultrahard nanomaterials based on MNF is that materials with the same hardness may differ in the elastic modulus (E), resistance against elastic strain to failure (H/E) and resistance against plastic deformation (H^3/E^2).[2]

E A Levashov, D V Shtansky Moscow State Institute of Steel and Alloys (Technology University), Leninsky prosp. 4, 119991 Moscow, Russian Federation. Fax (7-495) 952 53 08, tel. (7-495) 230 45 00, (7-495) 955 00 59, e-mail: levashov@shs.misis.ru (E A Levashov), tel. (7-495) 230 45 35, e-mail: shtansky@shs.misis.ru (D V Shtansky)

Received 10 November 2006
Uspekhi Khimii **76** (5) 501 – 509 (2007); translated by Z P Bobkova

Multifunctional nanostructured films are used to protect surfaces of articles and tools exposed simultaneously to elevated temperatures, corrosive media and various types of wear. This refers, first of all, to the cutting and press forming tools, mill rolls, parts of aircraft engines, gas turbines and compressors, friction bearings, glass and mineral fibre extrusion nozzles, *etc*. These films are also indispensable in the development of new-generation biocompatible materials, namely, orthopedic and dental implants, craniofacial and maxillofacial surgery implants, fixation of cervical and lumbar spines and so on.

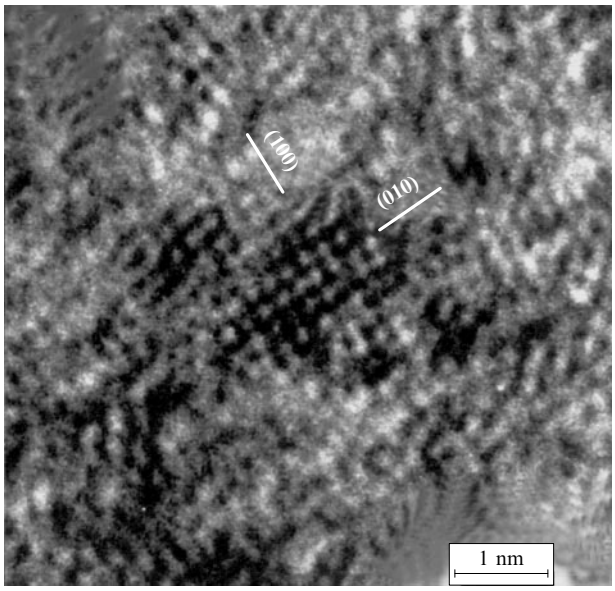


Figure 1. Crystallite with a 1.5 nm size in the Ti – Al – B – N film.[1]

Methods for the production of nanostructured materials and films and methods for the investigation of their structures, compositions, and properties have been widely addressed in Russian and foreign publications (see, for example, Refs 3 – 9).

† By changing the charge of the interfaces (by application of an electric field), one can affect the electronic structure of the films and, hence, their magnetic, optical and electric properties and also the mutual solubility of separate components and the formation of new phases.

This review presents a critical account of the promising trends in the application of MNF (based on refractory compounds) in mechanical engineering and medicine, *i.e.*, in those fields where the multifunctional properties of thin-film materials are manifested in full measure. Note that some MNF are used in other fields of technology, for example, in magnetooptics and electronics.

II. Multicomponent nanostructured films for mechanical engineering

Currently, titanium nitride-based films are widely used in industry. The introduction of a third component (for example, Si or B) into the films may markedly improve their physicomechanical properties and thus extend the scope of application. The interest in the Ti–Si–N films is mainly caused by their high hardness,[10–12] thermal stability,[13–15] resistance against high-temperature oxidation [14, 15] and substantial abrasive wear resistance.[16] Nanostructured Ti–B–N films possess a series of important performance characteristics including high hardness,[17–19] thermal stability up to 1000 °C (*in vacuo*),[20–22] heat,[15] wear [23–26] and corrosion resistance,[27] impact resistance [28] and high electrical resistance.[29] Chromium is known to have a beneficial effect on the stability of titanium carbides, borides and nitrides against oxidation [30] and on the wear resistance of articles made of them at elevated temperatures.[31]

Thus, the introduction of doping elements (Al, Si, B and Cr) into protective TiN films provides a combination of high hardness and wear resistance with relatively low friction coefficient (K_{fr}).[32, 33] In terms of their physicomechanical and tribological properties, MNF substantially surpass the conventional titanium nitride and carbonitride films. Thus the Ti–B–N and Ti–Cr–B–N films obtained under optimal conditions have hardnesses of 31–34 and 40–47 GPa, elastic moduli of 378 and 506 GPa, friction coefficients of 0.49–0.60 and 0.45–0.52, dry wear rates of $(3.4–4.6)\times10^{-7}$ and $(6.0–6.8)\times10^{-7}$ mm^3 N^{-1} min^{-1} and substrate adhesion (maximum critical load) of 50 and 42 N, respectively.[32]

The nanostructured films are prepared using both physical and chemical methods, among which physical vapour deposition methods (reactive and non-reactive magnetron deposition, cathode sputtering, laser ablation, *etc.*) are used most often. Ion plasma sputtering is an effective method for the synthesis of MNF. The use of multicomponent composite targets in the magnetron sputtering (MS) process and high-power metal ion beam-assisted MS gives nanostructured Ti–(Si,Cr,Al)–(B,N,C) coatings with controlled composition and high mechanical and tribological parameters.[33–36]

Coatings of the tribological use must possess high hardness, high fatigue strength and deformation and fracture resistance. All these requirements are satisfied for the tribological ultrahard ($H_v \geqslant 40$ GPa) nanostructured films composed of immiscible phases (or phases with limited mutual solubility), namely, nanocrystalline (*nc*) and amorphous (*a*) phases. The preparation of these films depends on the possibility of simultaneous deposition of nanocrystalline and amorphous phases. Transition metal nitrides (TiN, CrN, AlN, ZrN, TaN, *etc.*), carbides (TiC, VC, WC, ZrC, *etc.*), borides (TiB_2, CrB_2, WB, ZrB_2, *etc.*), oxides (Al_2O_3, TiO_2, SiO_2, MgO, Y_2O_3, ZrO_2, *etc.*) and silicides ($TiSi_2$, $CrSi_2$, $ZrSi_2$, *etc.*) are used as nanocrystalline phases, and Si_3N_4, BN, C and other substances can act as the amorphous matrices (Table 1).

Veprek *et al.*[14] proposed a theoretical concept for the design of ultrahard nanomaterials according to which these materials should be composed of dislocation-free nanocrystallites (solid phases) of 3–10 nm size separated by a thin (1–2 nm) amorphous phase layer. An idealised model of the ultrahard nanostructured film is shown in Fig. 2. It is noteworthy that complete phase segregation is usually observed when the films are deposited at high temperatures (500–600 °C), while upon deposition at lower temperatures, the interfaces may include both ordered and disordered sections, the amorphous phase being mainly formed as localised areas rather than as thin amorphous interlayers along the crystallite boundaries.[42]

It has been noted above that the hardness and the elasticity of nanostructured materials depend on the nanocrystallite size. The existence of the characteristic size of nanocrystallites (d_c) ensuring the highest hardness of nanostructured coatings is due to the continuous transition, at distances close to d_c, from the macroscopic dislocation nucleation and motion processes (for $d > d_c$) described by the known Hall–Petch law ($H \approx d^{-1/2}$) for conventional polycrystalline materials to intercrystallite local sliding processes along grain boundaries and interfaces (for $d < d_c$) .

Nanocrystallites with a size less than 10 nm are considered to contain no sources of generation of dislocations.[40] Note that the characteristic size of nanocrystallites as applied to nanocrystalline metallic materials can vary within 2–24 nm.[48] The

Table 1. Examples of tribological ultrahard nanostructured films consisting of immiscible phases.

Coating	Composition of the sputtered targets	Phase composition of films	Ref.
Ti–B–C–N	TiB + Ti or TiB_2 + TiC	*nc*-TiC + *nc*-TiB_2 + *a*-BN	37
Ti–B–N	TiB_2 + TiN or TiB_2 + Ti	*nc*-TiN + *nc*-TiB_2 (or *a*-TiB_2) + *a*-BN	33, 36, 38
Ti–Si–N	Ti_5Si_3 + Ti	*nc*-TiN + *nc*-$TiSi_2$ + *a*-Si_3N_4	39
	see [a]	*nc*-TiN + *a*-Si_3N_4	40
Ti–Cr–B–N	TiB + Ti_9Cr_4B + Cr_2Ti	*nc*-TiN + *nc*-CrB_2 + *a*-BN + *a*-TiB_2	33
Ti–C–B	TiC + TiB_2	*nc*-TiB_2 + *nc*-TiC + *a*-B_4C	41
Ti–Si–B–N	TiB_2 + Ti_5Si_3 + Si or TiB_2 + Si	*nc*-TiB_2 + *nc*-TiN + *nc*-$TiSi_2$ + *a*-Si_3N_4	35, 36
Ti–Si–C–N	TiC + Ti_5Si_3 or TiC + Ti_5SiC_2 + $TiSi_2$ + SiC	*nc*-TiC + *nc*-Ti_2SiC_2 + *nc*-$TiSi_2$ + *nc*-SiC + *a*-Si_3N_4	36, 42
Ti–Al–B–N	TiAlBN	*nc*-TiB_2 + *nc*-$(Ti_xAl_{1-x})N$ + *a*-BN + *a*-AlN	1
Ti–Al–C–N	TiAl + TiC	*nc*-TiC + *nc*-$(Ti_xAl_{1-x})N$ + *a*-AlN	36
W–C	W + laser ablation of C	*nc*-WC + *a*-C	43
W–Si–N	see [b]	*nc*-W_2N + *a*-Si_3N_4	44
Ti–C	$TiC_{0.5}$	*nc*-TiC + *a*-C	45
Ti–Al–Si–N	TiN + TiAl	*nc*-$(Ti_xAl_{1-x})N$ + *a*-Si_3N_4	46
Cr–Si–N	Cr + Si	*nc*-CrN + *a*-Si_3N_4	47
Cr–B–N	CrB_2	*nc*-CrB_2 + *a*-BN	33

Note. In most cases, films were prepared by magnetron sputtering from the targets in an Ar or N_2/Ar atmosphere. [a] The films were obtained by chemical vapour deposition (CVD). [b] The films were obtained by thermal annealing of the amorphous W–Si–N films.

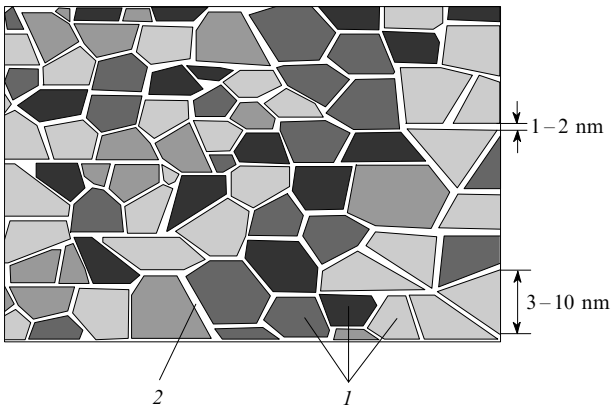


Figure 2. Idealised model of ultrahard nanostructured films. (*1*) Nanocrystalline phases, (*2*) amorphous phase.

experimental data on this issue available from the literature are rather scarce and contradictory. Thus a study of the structure of Ti – B – N films by high-resolution transmission electron microscopy [49] demonstrated the existence of a large number of internal edge dislocations in 5 – 15-nm crystallites. Figure 3 clearly shows the edge dislocation with the Burgers vector [100] within a 5-nm crystallite. Note also that the interfaces of nanostructured films often accommodate misfit dislocations (see Fig. 3), giving rise to long-range elastic stress fields.

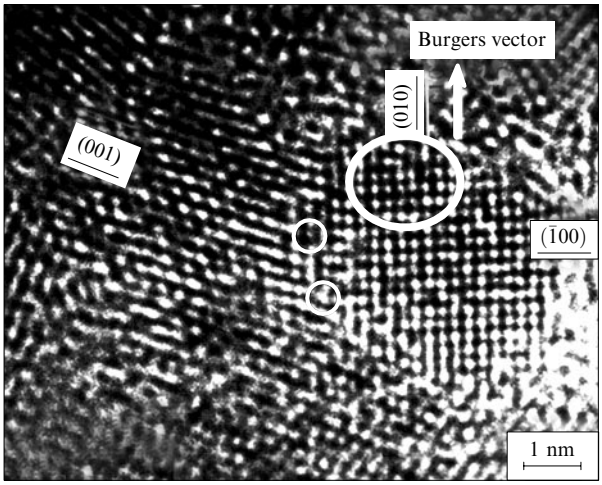


Figure 3. Edge dislocation inside the crystallite (large circle) and misfit dislocation at the crystallite boundary (small circles) in the Ti – Si – B – N film.[49]

The appearance of the amorphous phase in a nanostructured film is usually accompanied by a change in the film structure, namely, transition from the columnar structure,‡ representing a set of interconnected columns, to a composite structure in which nanocrystallites of one or several phases are separated by thin amorphous interlayers. Controlled introduction of 'amorphisers', for example, boron or silicon, allows targeted variation of the structure and properties of nanostructured films. Thus the highest hardness of M – Si – N films (M is a transition metal) was attained in composite nanostructured *nc*-MN + *a*-Si_3N_4 films with the characteristic crystallite size $d_c \approx 10$ nm at a silicon content within the 7 at.% – 10 at.% range.[50]

Although the reasons for ultrahigh hardness of some composites are not fully understood, the key factors favourable for the increase in hardness can be listed. These include high compression stresses arising due to the difference between the thermal expansion coefficients of the substrate and the coating; distortion of the crystal phase lattice caused by the change in the mutual solubility of elements; high internal stress (or growth stress) and chemical bonds between some phase components.

In addition to high hardness, tribological nanostructured films are expected to have low elastic moduli and high elastic recovery values (W_e), reaching 90%. The numerical values of these characteristics can be measured using a nanohardness tester. Using known parameters E and W_e, one can calculate H/E and H^3/E^2. The dependences $H = f(E^*)$ [$E^* = E(1 - \nu^2)$ is the effective elastic modulus, where ν is the Poisson coefficient], $H^3/E^2 = f(H)$ and $W_e = f(H)$ are the principal relations describing the mechanical properties of the films.[51]

For a series of oxide, carbide, nitride and composite nanostructured films obtained by magnetron sputtering, the dependence $H = f(E^*)$ can be approximated by a straight line, while the dependence $H^3/E^2 = f(H)$, by a parabola.[44, 45]

$$H = 0.15\,E^* - 12,$$

$$\frac{H^3}{E^2} = 4.3 \times 10^{-4}\,H^2.$$

These equations are useful for predicting the mechanical behaviour of films.

Plastic deformation (W_p) is yet another important chracteristics of nanostructured films. No quantitative relationship (as approximating equations) exists between the W_p, H and H^3/E^2 values,[52] but only a qualitative relationship. As H and H^3/E^2 increase, the W_p value decreases; films with $H > 25$ GPa have relatively low plastic deformation values ($\sim 30\%$).

The local deformation mechanisms in nanostructured thin films have been investigated.[19, 53] The existence of two local deformation mechanisms for such films was established, namely, homogeneous (with weak chemical bonds between structural elements) and non-homogeneous (with strong bonds between the crystallites). Both deformation mechanisms are implemented by sliding of the structure elements, *i.e.*, separate grains (homogeneous mechanism) or multigrain domains (columnar elements) (non-homogeneous mechanism), parallel to the applied load. In the case of weak chemical bonds between the neighbouring grains, some structure elements can be expelled to the outside as a result of elastic stress relaxation upon load release. In the case of strong chemical bonds between neighbouring grains, the deformation occurs through sliding of the columnar elements, resulting in the formation of shear steps.

The tribological properties of films largely depend on the phase composition of the nanocomposite. Thus for the Ti – B – N and Ti – Cr – B – N films, the friction coefficient decreases to 0.40 with a decrease in the boron content and an increase in the nitrogen content. This low K_{fr} value is due to the presence of the hexagonal *a*-BN phase.[33] The presence of silicon also enhances the tribological properties of nanostructured films. For example, the friction coefficient of the Ti – Si – B – C – N films in the friction couple with a WC – Co carbide ball decreases to 0.15 as the silicon concentration grows to 12 at.%. Silicon promotes the formation of intermediate solid lubricant layers resulting from tribochemical reactions during friction. Silicon compounds such as $TiSi_2$, SiC and SiB_4 as the film constituents are known to react with water

‡ It is believed that undesirable stresses parallel to the substrate surface arise in the films with columnar structure.

and oxygen to give self-lubricated tribolayers of the SiO_2 or $Si(OH)_4$ type.

An enhanced wear resistance of a material can also be indicated by high values of H/E. This correlation has been confirmed both theoretically and experimentally for a large number of materials.[54]

A number of publications[43,55,56] describe the first synthesis of 'chameleon' type nanostructured films. These tribological nanocomposite films with low K_{fr} values represent mixtures of hard and soft self-lubricated phases. The hard phases (nitrides, carbides or boride) are responsible for high wear resistance under high load, while soft phases (a-C, a-WS_2, a-Si_3N_4, a-BN) significantly decrease K_{fr} of the contact friction couple.

Sputtering of multilayer or functionally gradient nanostructured films with alternating ultrahard and self-lubricated layers is a promising trend in the design of tribological coatings with ultimately low K_{fr} values (< 0.05). As an example, consider bilayer WSe_x/TiC, WSe_x/TiCN and WSe_x/TiSiN films in which the WSe_x layer consists of WSe_2 and W_3O nanocrystalline phases incorporated in the amorphous a-WSe_x matrix.[57] These bilayer compositions had a low friction coefficient both in air ($K_{fr} = 0.015-0.05$) and in water ($K_{fr} = 0.06-0.07$) throughout the whole series of tribological investigations. A distinctive feature of these films is the absence of starting (break-in) friction coefficient in the beginning of testing, which is usually the highest.

An important factor for increasing the service life of articles at high temperatures is to ensure their thermal stability and high-temperature oxidation resistance (heat resistance). These parameters depend on the elemental and phase composition of the films and on the thermal stability of the constituent individual phases. The thermal stability of nanostructured films has been considered in detail in a review by Andrievskii.[58]

As an example, Fig. 4 shows the dependence of the average crystallite size in nanostructured Ti–B–N and Ti–Cr–B–N films on the annealing temperature. It can be seen that the average size of crystallites does not exceed 5 nm even after annealing of the films *in vacuo* at 1000 °C for 1 h. The same figure shows the dependence of film hardness on the annealing temperature. Both films showed an increase in hardness with an increase in the annealing temperature to 800 °C; for the Ti–Cr–B–N films, this high hardness was retained up to 1000 °C, the hardness of the Ti–B–N films at 1000 °C was somewhat lower than at 800 °C but nevertheless it was rather high.[33] This extremal pattern of hardness variation with temperature is in good agreement with previous results, indicating the presence of a hardness peak for the Ti–Al–Si–N[59] and W–Si–N films[60] at 800 and 900–950 °C, respectively.

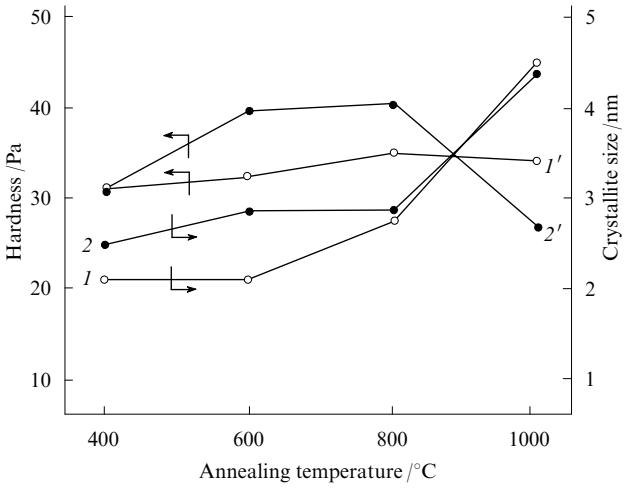


Figure 4. Average size of crystallites (curves *1*, *2*) and hardness (curve *1′*, *2′*) of the Ti–Cr–B–N (*1*, *1′*) and Ti–B–N (*2*, *2′*) films *vs.* annealing temperature.

The microcrystalline TiN, TiC, TiCN and TiAlN films obtained by physical deposition are known to demonstrate a monotonic decrease in hardness with an increase in temperature.[61,62] The increase in the hardness of nanostructured films with the increase in temperature may be due to the change in the thickness of intergrain amorphous interlayers and the concentration-induced separation of metastable phases.[7] In addition, hardness can be affected by stoichiometry of the crystalline phase. Thus the maximum hardness of the Ti–Si–B–N films was achieved at the strictly stoichiometric composition of the $Ti(B,N)_2$ phase.[63]

In some publications (see, for example, Ref. 12), it was suggested that the high hardness of the nanostructured films obtained by low-temperature magnetron sputtering is related to the presence of high compression stresses. As the temperature is increased (to 450 °C), elastic stress relaxation takes place and, as a consequence, the hardness of films decreases down to values typical of polycrystalline materials. However, this assumption is at variance with the data obtained for nanostructured Ti–B–N and Ti–Cr–B–N films; these films retain high hardness up to 1000 °C.

The heat resistance of the films has a critical temperature above which the film is completely oxidised and destroyed. The heat resistance varies over a broad range from 400 to 950 °C (Table 2). A common feature of nanostructured films is the polycrystalline structure, which provides direct oxygen access to the substrate along the grain boundaries (by the surface reactive diffusion mechanism). This accounts for the relatively low heat resistance of polycrystalline films.

An efficient way for increasing the heat resistance of solid films is suppression of the recrystallisation of nanocrystallites by creating a dense composite structure in which the crystallites occur in the amorphous matrix containing elements (Si, Al, Cr, B) with high oxygen affinity. It has been shown[67–70] that the nc-MN_x + a-Si_3N_4 (M = Ta, Zr, Mo) compositions with high (> 50 at.%) contents of the amorphous phase meet these requirements. These films have a high heat resistance (~1000 °C), while retaining high hardness within the 20–40 GPa range.

The positive influence of amorphising elements (Si, Al and B) on the heat resistance of nanostructured Ti–B–N, Ti–Si–B–N, Ti–Si–C–N, Ti–Al–C–N and Ti–C–B films is manifested as an increase in the content of amorphous phases (a-Si_3N_4, a-AlN, a-BN, a-B_4C); an increase in the thermal stability of the nanocrystalline state; the formation of a protective oxide layer on the film surface preventing the oxygen access to the substrate.[36,41,71–74] For example, in the $(Ti,Al)_{1-x}(C,N)_x$ nanostructured films, oxygen is dissolved in

Table 2. Heat resistance of some nanostructured films.

Film	Heat resistance /°C	Ref.
TiC	400	64
TiN	650	30
TiAlN	850	30
(Ti,Al,Y)N	950	65
MSiN [a] (M = Ti, Zr, Cr, W, Ta, Mo, Nb)	950	66

[a] The silicon content does not exceed 10 at.%.

the fcc lattice at 800 °C,§ while at 1000 °C, aluminium diffuses toward the film surface to form a protective Al_2O_3 layer, which prevents further oxidation.

The results of measurements of the oxidation depth of nanostructured Ti–B–N and Ti–Si–B–N films at various temperatures are presented in Fig. 5. It can be seen that the oxidation resistance of Ti–B–N and Ti–Si–B–N films is higher than that of TiN films, which are oxidised to depth of 800 nm at 550 °C. The Ti–Cr–B–N and Ti–Al–Si–B–N films are even more resistant against high-temperature oxidation: the depth of oxygen penetration into these films did not exceed 800 nm even after annealing at 800 °C. The high heat resistance of the Ti–Cr–B–N and Ti–Al–Si–B–N films is due to the formation of $(Ti,Cr)BO_3$ and $Ti_xAl_ySiO_z$ oxide–based protective layers on their surfaces. In terms of the high-temperature oxidation resistance, these films can be arranged in the order TiN > Ti–B–N > Ti–Si–B–N > Ti–Cr–B–N > Ti–Al–Si–B–N (the authors' data).

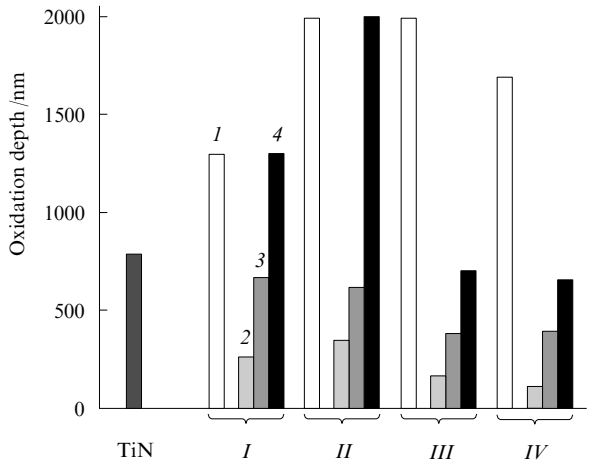


Figure 5. Oxidised layer thickness in the Ti–B–N (*I*), Ti–Si–B–N (*II*), Ti–Cr–B–N (*III*) and Ti–Al–Si–B–N (*IV*) films *vs.* annealing temperature. For comparison, the oxidation depth for the TiN coating after annealing at 550 °C is given.
(*1*) Film thickness, (*2*) thickness of the oxidised layer after film annealing at a temperature of 600 °C, (*3*) the same at 700 °C, (*4*) at 800 °C.

For a number of practical applications, for example, for high-speed cutting or for mechanical tooling in a fluid lubricant, it is important that the films combine high heat resistance with corrosion resistance. The electrochemical testing of the Ti–B–N films carried out in 1 N H_2SO_4 at room temperature demonstrated advantages of chromium-doped films over non-doped or silicon- and aluminium-doped films.[36] The Ti–Cr–B–N films have greater positive free corrosion potentials and fourfold lower current density (corrosion rate at the passivation potential) compared to those of the Ti–B–N films, whereas the Ti–Si–B–N and Ti–Al–Si–B–N films have low corrosion and passivation resistances. The corrosion rates of the Ti–Si–B–N and Ti–Al–Si–B–N films under passivation conditions were 6.6 and 14 times higher, respectively, and the free corrosion potentials were more negative than those of the Ti–B–N film. This experiment shows that introduction of chromium in the Ti–B–N films results in stabilisation of the protective oxide layer on the film surface under anodic polarisation conditions.

§ A 800-nm thick titanium oxide layer is formed on the surface of the standard titanium nitride film under the same conditions.

The above data indicate that the progress in the design of solid wear-resistant nanostructured coatings implies imparting qualitatively new properties and multifunctional character to these coatings. In addition to high hardness and wear resistance, these coatings have low friction coefficients, and high thermal stability and heat and corrosion resistances.

III. Multifunctional nanostructured films for medicine

A topical scientific and technological task of modern biology and materials science is the design of new biomaterials able to accelerate the adaptation of artificial implants to living tissues and markedly increase their service life. The complexity of the problem is due to the fact that none of the materials currently used to produce implants possesses all properties of the bone tissue. New biomaterials for implants should combine the advantages of various materials, in particular, biocompatibility, bioactivity, corrosion stability in physiological media, high fatigue strength and rupture strength, low elastic modulus and friction coefficient, high wear resistance.

Metals and alloys are used most often to produce implants. The use of titanium, stainless steel 316-L and the Cr–Co–Mo alloy (vitallium) in medical practice for the manufacture of implants started back in 1937. However, pure titanium has a relatively low wear resistance; therefore, in medicine it has been replaced by the Ti–Al–V alloys, which are not only biocompatible but also show high mechanical strength, corrosion resistance, fatigue strength and wear resistance. However, the toxicity of vanadium and the side effects caused by the presence of aluminium ions (high risks of thrombus formation and neural disorder) restrict the use of Ti–Al–V alloys in medicine.[75,76] In order to eliminate the adverse effect of Al and V ions, new titanium alloys were developed, *e.g.*, Ti–Nb–Zr[75] and Ti–In–Nb–Ta.[77]

The Ni–Ti, Ni–Cr–Mo and Au–Pt alloys and BT1-0, BT5 and BT14 titanium alloys are often used in medicine. Note that the metal or alloy surface is bioinert and cannot adsorb biological molecules or form chemical bonds with living tissues; therefore, in order to increase the bioactivity of metals and alloys, a hydroxyapatite layer [$Ca_{10}(PO_4)_6(OH)_2$, HAP], is often applied on their surface.¶ Unfortunately, HAP cannot be applied on the surfaces of implants operating under load, as it has low strength and crack resistance compared to those of bone tissue.[78,79]

Yet another class of materials widely used in medicine includes ceramic materials TiN, TiO_2, SiO_2, Al_2O_3, ZrO_2 and SiC. Thus owing to its excellent mechanical properties, zirconia-based ceramics has been used in endoprosthesis replacement (as parts of artificial joints and couplings) since the late 1960s.[80,81] In 2003, the United States Food and Drug Administration (FDA) approved the use of Al_2O_3 in medicine. However, neither ZrO_2 nor Al_2O_3 can form chemical bonds with the bone tissue. Ceramics based on TiN is better suited for medical purposes. Titanium nitride (as a thin coating) is widely used to protect the surface of dentures, artificial hip joints and cardiac valves.[82–85] This is due to the combination of several useful properties in TiN films, *e.g.*, high hardness, relatively high corrosion stability and biocompatibility. In addition, TiN (Refs 86, 87) and TiO_2 (Ref. 88) films possess high hemocompatibility. However, TiN has a too high friction coefficient and too low wear resistance to ensure a long service life. It is significant to note that SiO_2 and TiO_2 coatings have a negatively charged surface within the human body (environ-

¶ A layer of HAP and calcium phosphate is often used as a bioactive boundary between the implant and the surrounding tissue due to the close similarity of their chemical and mineral components.

ment acidity pH 7), resulting in the formation of a hydroxyapatite layer.[89] Amorphous silicon carbide-based alloys are used to improve the biocompatibility of artificial cardiac valves.[90] The drawbacks of the ceramics include enhanced brittleness, high elastic modulus and low bioactivity if any.

Carbon-based coatings deserve special note. Diamond-like carbon, a metastable form of amorphous carbon containing a considerable number of $C(sp^3)-C(sp^3)$ bonds, is a solid wear- and corrosion-resistant material with a low friction coefficient, chemical inertness and biocompatibility.[91,92]

Bioactive ceramics initiates the formation of a bone-like apatite layer on its surface, and through this layer the material is bound to the bone tissue. The formation of an apatite layer on the ceramic surface is possible if the ceramics contains some Ca, Si, P, C and O atoms.[93,94] The formation of an apatite layer is related to the formation of OH groups on the charged surface of bioactive ceramics in the living organism.[95–97] The silicate ceramics $CaO-SiO_2$ (Refs 95 and 96) and $CaO-MgO-2\,SiO_2$ (Ref. 98) show good bioactivity and biocompatibility. The introduction of bioinert additives such as ZrO_2 into the bioactive matrix may improve mechanical properties.[99] A drawback of this ceramics is enhanced brittleness, high elastic modulus, limited plasticity and low cracking resistance.

A possible way of improving the properties of metallic implants operating under load is their coating with protective films with multifunctional properties. Recently a fundamentally new approach to the design of biocompatible thin-film materials has been developed; according to this approach, additional elements (Ca, Zr, Mn, O, P) are introduced into titanium carbide-, carbonitride- or silicide-based films to improve the mechanical and tribological properties of the material and ensure the bioactive properties and biocompatibility of the surface.[100–104] Inorganic additives, CaO, ZrO_2, TiO_2, $KMnO_4$ and HAP, are introduced during the self-propagating high-temperature synthesis (SHS) of composite targets, which are subsequently used for the ion plasma film deposition. The use of high-power metal ion beam-assisted magnetron sputtering of such composite targets allows one to modify the surface of the metallic implants. This process gives dense films with high adhesion strength and controlled elemental composition. The nanocomposite $TiC-CaO$ films can also be manufactured by a mixed PVD/PACVD process, which represents a combination of the magnetron sputtering from a composite target $TiC_{0.5}$ + CaO and plasma assisted chemical vapour deposition (PACVD). The activated plasma is used to increase the ionisation degree of the sputtered particles.[105–108]

Since the bulk ceramic materials have high Young modulus and rather low plasticity, their deformation is accompanied by the formation and propagation of cracks resulting in fast destruction of the material. An important advantage of MNF is that they possess high hardness and rather low elastic modulus, which is much lower than that of Al_2O_3, TiN, SiC or ZrO_2 ceramic materials. The low Young modulus of the MNF, similar to that of bone tissue (30 GPa), results in a better bearing of functional loads by a bone tissue and stimulates growth of the bone tissue. Thus, MNF represent a new unique type of material for medical applications combining high hardness with elastic recovery. Whereas the H^3/E^2 parameter of bulk ceramics (TiN, TiO_2, SiO_2 ZrO_2 and SiC) does not exceed 0.2 GPa, in the case of MNF, it varies from 0.1 to 0.9 GPa. Multifunctional nanostructured films exhibit high resistance against elastic strain to failure as compared with bulk ceramics.[54] The H/E parameter is also a measure of the wear resistance of a material.[109]

The biocompatibility of new materials is now estimated by two types of testing, first, studies of the *in vitro* cytocompatibility (cytotoxicity) and of the *in vivo* biocompatibility. The adhesion of cells followed by spreading on the implant surface is the first stage of interaction between the organism cells and the implant. This stage is crucial, as this determines the material biocompatibility. The shape and degree of cell spreading on the substrate depends on the actinic cytoskeleton. Since artificial implants are used most often to replace the bone tissue, of particular interest is their interaction with fibroblasts (connective tissue cells) and osteoblasts (bone tissue cells). The effective spreading of cells is necessary for proliferation and, in the case of osteoblasts, for the subsequent differentiation resulting in the formation of bone tissue from hydroxyapatite.[110]

Effective implantation requires integration of the implants into the tissue medium and their firm connection to the bone without interlayers, *i.e.*, osteointegration. The effect of the implant material on the capability of bone cells (osteoblasts) for differentiation is estimated in *in vitro* experiments using various cell systems, for example, MC3T3-E1 mice osteoblasts or primary cultures of rat osteoblasts isolated from newborn animals.

The biocompatibility is usually estimated in *in vivo* studies by hypodermic implantation of the materials tested in animals.[100,101] These studies are necessary, first of all, because the implantation of artificial materials in a living organism usually induces acute and chronic inflammatory processes, the degree of which depends directly on the biocompatibility of the implants. The inflammatory responses are due to polymorphonuclear leucocytes (neutrophiles) and lymphocytes, which are accumulated in the inflamed area. Macrophages are also accumulated on the surface of the foreign object; they can be combined to form multinucleate giant cells. It is considered that these giant cells of foreign objects are most active and play the crucial role in the implant destruction.[111] The activated macrophages produce cytokines (TNFα), which accumulate neutrophiles and lymphocytes, promoting the inflammation.[112] Macrophages can release osteoinductive signals, in particular, bone morphogenetic proteins.[111,112] Bone osteoinductive proteins are known to stimulate the differentiation of osteoblasts and the formation of bone tissue.[113] The amount of macrophages, neutrophiles, lymphocytes and multinucleate giant cells on the implant surface is an important characteristics for the estimation of biocompatibility of the studied materials.

The osteointegration process is evaluated by implanting the tested materials into the bone tissue of laboratory animals. The degree of osteointegration is judged by the degree of resorption of the bone material around the implant, the structure and the maturity of the connective tissue and the newly formed cell structures. Figure 6 shows the interface between the bone and

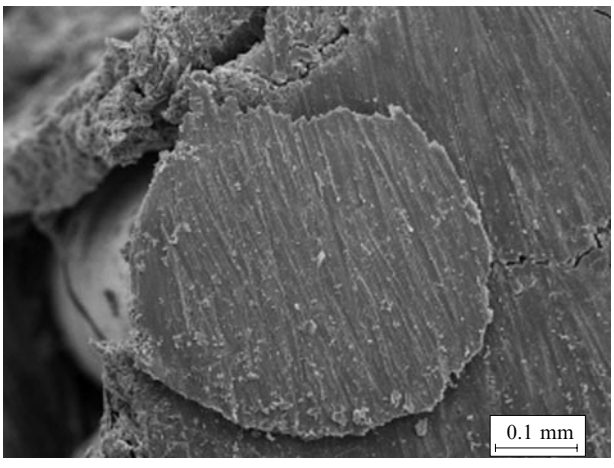


Figure 6. Interface between the bone and the titanium implant surface with the nanostructured $Ti-Ca-P-C-O-N$ coating.

the titanium implant surface with the nanostructured Ti–Ca–P–C–O–N coating 30 days after the implantation. One can see areas of tight contact between the implant and the bone without the formation of coarse-fibred structures, gaps or voids.

The biocompatible MNF obtained to date have high hardnesses (25–40 GPa) and adhesion strengths (critical load > 30 GPa), low elastic moduli (150–250 GPa), low friction coefficients (0.1–0.25) and wear rates ($< 10^{-5}$ $mm^3\ N^{-1}\ min^{-1}$) in physiological media, high resistances against elastic strain to failure (> 0.1) and plastic deformation (> 0.2 GPa). They are characterised by negative charge on the surface at the acidity of the medium of pH 6–8, surface hydrophilicity and bioactivity, biocompatibility and accelerated osteointegration.[100, 101]

Thus, MNF have a number of advantages over known bulk and thin-film analogues, which makes them promising materials for implants operating under load.

References

1. D V Shtansky, K Kaneko, Y Ikuhara, E A Levashov *Surf. Coat. Technol.* **148** 206 (2001)
2. D V Shtansky, S A Kulinich, E A Levashov, J J Moore *Fiz. Tv. Tela* **45** 1122 (2003) [a]
3. *Nanostructured Coatings* (Eds A Cavaleiro, J T De Hosson) (Berlin: Springer, 2006)
4. P H Mayrhofer, C Mitterer, L Hultman, H Clemens *Prog. Mater. Sci.* **51** 1032 (2006)
5. R A Andrievskii *Usp. Khim.* **74** 1163 (2005) [*Russ. Chem. Rev.* **74** 1061 (2005)]
6. S Veprek, M G J Veprek-Heijman, P Karvankova, J Prochazka *Thin Solid Films* **476** 1 (2005)
7. *Nanostructured Thin Films and Nanodispersion Strengthened Coatings* (Eds A A Voevodin, D V Shtansky, E A Levashov, J J Moore) (Dordrecht: Kluwer Academic, 2004)
8. R A Andrievskii *Ros. Khim. Zh.* **46** (5) 50 (2002) [b]
9. D V Shtansky *Ros. Khim. Zh.* **46** (5) 81 (2002) [b]
10. P Jedrzejowski, J E Klemberg-Sapieha, L Martinu *Thin Solid Films* **426** 150 (2003)
11. P J Martin, A Bendavid *Surf. Coat. Technol.* **163–164** 245 (2003)
12. S Veprek, A S Argon *J. Vac. Sci. Technol., B* **20** 650 (2002)
13. H-D Männling, D S Patil, K Moto, M Jilek, S Veprek *Surf. Coat. Technol.* **146–147** 263 (2001)
14. S Veprek, M Haussmann, S Reiprich, L Shizhi, J Dian *Surf. Coat. Technol.* **86–87** 394 (1996)
15. S Veprek *J. Vac. Sci. Technol., A* **17** 2401 (1999)
16. M Diserens, J Patscheider, F Lévy *Surf. Coat. Technol.* **108–109** 241 (1998)
17. P Losbichler, C Mitterer, P N Gibson, W Gissler, F Hofer, P Warbichler *Surf. Coat. Technol.* **94–95** 297 (1997)
18. S Veprek, P Nesladek, A Niederhofer, F Glatz, M Jilek, M Sima *Surf. Coat. Technol.* **108–109** 138 (1998)
19. R A Andrievski, G V Kalinnikov *Surf. Coat. Technol.* **142–144** 573 (2001)
20. R A Andrievskii, G V Kalinnikov, A E Oblezov, D V Shtansky *Dokl. Akad. Nauk* **384** 36 (2002) [c]
21. P Karvankova, M G J Veprek-Heijman, O Zindulka, A Bergmaier, S Veprek *Surf. Coat. Technol.* **163–164** 149 (2003)
22. C Mitterer, P H Mayrhofer, J Musil *Vacuum* **71** 279 (2003)
23. D V Shtansky, E A Levashov, N N Khavskii, J J Moore *Izv. Vyssh. Uchebn. Zaved., Tsv. Metallurg.* (1) 59 (1996)
24. J L He, S Miyake, Y Setsuhara, I Shimizu, M Suzuki, K Numata, H Saito *Wear* **249** 498 (2001)
25. C Héau, J P Terrat *Surf. Coat. Technol.* **108–109** 332 (1998)
26. M Stoiber, C Mitterer, T Schoeberl, E Badisch, G Fontalvo, R Kullmer *J. Vac. Sci. Technol., B* **21** 1084 (2003)
27. M Tamura, H Kubo *Surf. Coat. Technol.* **54–55** 255 (1992)
28. C Rebholz, H Ziegele, A Leyland, A Matthews *J. Vac. Sci. Technol., A* **16** 2851 (1998)
29. R A Andrievskii, G V Kalinnikov, N P Kobelev, Ya M Soifer, D V Shtanckii *Fiz. Tv. Tela* **39** 1859 (1997) [a]
30. L A Donohue, I J Smith, W-D Münz, I Petrov, J E Greene *Surf. Coat. Technol.* **94–95** 226 (1997)
31. E Pflüger, A Schröer, P Voumard, L Donohue, W-D Münz *Surf. Coat. Technol.* **115** 17 (1999)
32. D V Shtansky, A N Sheveiko, M I Petrzhik, F V Kiryukhantsev-Korneev, E A Levashov, A Leyland, A L Yerokhin, A Matthews *Surf. Coat. Technol.* **200** 208 (2005)
33. D V Shtansky, F V Kiryukhantsev-Korneev, A N Sheveiko, I A Bashkova, O V Malochkin, E A Levashov, N B D'yakonova, I V Lyasotskii *Fiz. Tv. Tela* **47** 242 (2005) [a]
34. F V Kiryukhantsev-Korneev, D V Shtansky, A N Sheveiko, E A Levashov, I V Lyasotskii, N B D'yakonova *Fiz. Met. Metalloved.* **97** 96 (2004) [d]
35. D V Shtansky, E A Levashov, A N Sheveiko, J J Moore *J. Mater. Synth. Process.* **7** 187 (1999)
36. D V Shtansky, E A Levashov, A N Sheveiko, J J Moore *J. Mater. Synth. Process.* **6** 61 (1998)
37. O Knotek, R Breidenbach, F Jungblut, F Löffler *Surf. Coat. Technol.* **43–44** 107 (1990)
38. C Mitterer, M Rauter, P Rödhammer *Surf. Coat. Technol.* **41** 351 (1990)
39. D V Shtansky, I V Lyasotsky, N B Dyakonova, F V Kiryukhantsev-Korneev, S A Kulinich, E A Levashov, J J Moore *Surf. Coat. Technol.* **182** 204 (2004)
40. S Veprek, S Reiprich *Thin Solid Films* **268** 64 (1995)
41. E A Levashov, V I Kosayanin, L M Krukova, J J Moore, D L Olson *Surf. Coat. Technol.* **92** 34 (1997)
42. D V Shtansky, E A Levashov, A N Sheveiko, J J Moore *Metall. Mater. Trans., A* **30** 2439 (1999)
43. A A Voevodin, J P O'Neill, S V Prasad, J S Zabinski *J. Vac. Sci. Technol., A* **17** 986 (1999)
44. C Louro, A Cavaleiro, S Dub, P Smid, J Musil, J Vlcek *Surf. Coat. Technol.* **161** 111 (2002)
45. M Stüber, H Leiste, S Ulrich, H Holleck, D Schild *Surf. Coat. Technol.* **150** 218 (2002)
46. S Carvalho, L Rebouta, E Ribeiro, F Vaz, M F Denannot, J Pacaud, J P Rivière, F Paumier, R J Gaboriaud, E Alves *Surf. Coat. Technol.* **177–178** 369 (2004)
47. E Martinez, R Sanjinés, A Karimi, J Esteve, F Lévy *Surf. Coat. Technol.* **180–181** 570 (2004)
48. V G Gryaznov, I A Polonsky, A E Romanov, L I Trusov *Phys. Rev., B* **44** 42 (1991)
49. R A Andrievskii, G V Kalinnikov, D V Shtansky *Fiz. Tv. Tela* **42** 741 (2000) [a]
50. J Musil, S Miyake *Novel Materials Processing by Advanced Electromagnetic Energy Sources (MAPEES'04)* (Amsterdam: Elsevier, 2005) p. 345
51. J Musil *Surf. Coat. Technol.* **125** 322 (2000)
52. J Musil, F Kunc, H Zeman, H Poláková *Surf. Coat. Technol.* **154** 304 (2002)
53. D V Shtansky, S A Kulinich, E A Levashov, A N Sheveiko, F V Kiriuhancev, J J Moore *Thin Solid Films, C* **420–421** 330 (2002)
54. A Leyland, A Matthews *Wear* **246** 1 (2000)
55. A A Voevodin, J J Hu, T A Fitz, J S Zabinski *J. Vac. Sci. Technol., A* **20** 1434 (2002)
56. A A Voevodin, J S Zabinski *Thin Solid Films* **370** 223 (2000)
57. D V Shtansky, T A Lobova, V Yu Fominski, S A Kulinich, I V Lyasotsky, M I Petrzhik, E A Levashov, J J Moore *Surf. Coat. Technol.* **183** 328 (2004)
58. R A Andrievskii *Usp. Khim.* **71** 967 (2002) [*Russ. Chem. Rev.* **71** 853 (2002)]
59. S Veprek, H-D Mannling, M Jilek, P Holubar *Mater. Sci. Eng., A* **366** 202 (2004)
60. A P Marques, A Cavaleiro *Thin Solid Films* **441** 150 (2003)
61. L Karlsson, A Horling, M P Johansson, L Hultman, G Ramanath *Acta Mater.* **50** 5103 (2002)
62. S PalDey, S C Deevi *Mater. Sci. Eng., A* **342** 58 (2003)
63. D V Shtansky, E A Levashov, A N Sheveiko, J J Moore *Izv. Vyssh. Uchebn. Zaved., Tsv. Metallurg.* (1) 67 (1999)
64. W D Münz *J. Vac. Sci. Technol., A* **4** 2717 (1986)

65. I Wadsworth, I J Smith, L A Donohue, W-D Münz *Surf. Coat. Technol.* **94 – 95** 315 (1997)
66. S Veprek, M Hausmann, S Reiprich *Mater. Res. Soc. Symp. Proc.* **400** 261 (1996)
67. H Zeman, J Musil, P Zeman *J. Vac. Sci. Technol., A* **22** 646 (2004)
68. J Musil, R Daniel, P Zeman, O Takai *Thin Solid Films* **478** 238 (2005)
69. J Musil, P Dohnal, P Zeman *J. Vac. Sci. Technol., B* **23** 1568 (2005)
70. P Zeman, J Musil, R Daniel *Surf. Coat. Technol.* **200** 4091 (2006)
71. D Zhong, J J Moore, B M Mishra, T Ohno, E A Levashov, J Disam *Surf. Coat. Technol.* **163 – 164** 50 (2003)
72. D V Shtansky, E A Levashov, A N Sheveiko *Galvanotechnik* **88** 3368 (1997)
73. D V Shtansky, E A Levashov, A N Sheveiko, J J Moore *Int. J. Self-Propag. High-Temp. Synth.* **7** 249 (1998)
74. Y Tanaka, T M Gur, M Kelly *J. Vac. Sci. Technol., A* **10** 1749 (1992)
75. J A Davidson, A K Mishra, P Kovacs, R A Poggie *Biomed. Mater. Eng.* **4** 231 (1994)
76. S J Lugowski, D C Smith, A D McHugh, J C Van Loon *J. Biomed. Mater. Res.* **25** 1443 (1991)
77. B-H Lee, Y D Kim, K H Lee *Biomaterials* **24** 2257 (2003)
78. S F Hulbert, F A Young, R S Mathews, J J Klawitter, C D Talbert, F H Stelling *J. Biomed. Mater. Res.* **4** 433 (1970)
79. L L Hench *J. Am. Ceram. Soc.* **74** 1487 (1991)
80. C Piconi, G Maccauro *Biomaterials* **20** 1 (1999)
81. E Adolfsson, L Hermanson *Biomaterials* **20** 1263 (1999)
82. P V Kola, S Daniels, D C Cameron, M S J Hashmi *J. Mater. Process. Technol.* **56** 422 (1996)
83. S Mändl, B Rauschenbach *Surf. Coat. Technol.* **156** 276 (2002)
84. P A Dearnley *Proceedings of the Institution of Mechanical Engineers, Part H (J. Eng. Med.)* Vol. 213 (London: Professional Eng. Publ., 1999) p. 107
85. S Piscanec, L C Ciacchi, E Vesselli, G Comelli, O Sbaizero, S Meriani, A de Vita *Acta Mater.* **52** 1237 (2004)
86. I Dion, X Roques, N More *Biomaterials* **14** 712 (1993)
87. J J A M Van Raay, P M Rozing, C A Van Blitterswijk, R M Van Haastert, H K Koerten *J. Mater. Sci.: Mater. Med.* **6** 80 (1995)
88. N Huang, P Yang, Y X Leng, J Y Chen, H Sun, J Wang, G J Wang, P D Ding, T F Xi, Y Leng *Biomaterials* **24** 2177 (2003)
89. P J Li, C Ohtsuki, T Kokubo, K Nakanishi, N Soga, K de Groot *J. Biomed. Mater. Res.* **28** 7 (1994)
90. A Bolz, M Schaldach *Artif. Organ.* **14** 260 (1990)
91. R Hauert *Diamond Relat. Mater.* **12** 583 (2003)
92. A Grill *Diamond Relat. Mater.* **12** 166 (2003)
93. S H Maxian, J P Zawadsky, M G Dunn *J. Biomed. Mater. Res.* **28** 1311 (1994)
94. X Y Liu, P K Chu, C X Ding *Mater. Sci. Eng., R* **47** 49 (2004)
95. P N De Aza, Z B Luklinska, M R Anseau, M Hector, F Guitivn, S De Aza *Biomaterials* **21** 1735 (2000)
96. T Kokubo, H-M Kim, M Kawashita *Biomaterials* **24** 2161 (2003)
97. P Li, I Kangasniemi, K De Groot *Bioceramics* **6** 41 (1993)
98. T Nonami, S Tsutsumi *J. Mater. Sci.: Mater. Med.* **10** 475 (1999)
99. H Ji, P M Marquis *Biomaterials* **13** 744 (1992)
100. D V Shtansky, N A Gloushankova, I A Bashkova, M A Kharitonova, T G Moizhess, A N Sheveiko, F V Kiryukhantsev-Korneev, M I Petrzhik, E A Levashov *Biomaterials* **27** 3519 (2006)
101. D V Shtansky, N A Gloushankova, A N Sheveiko, M A Kharitonova, T G Moizhess, E A Levashov, F Rossi *Biomaterials* **26** 2909 (2005)
102. D V Shtansky, E A Levashov, N A Glushankova, N B D'yakonova, S A Kulinich, M I Petrzhik, F V Kiryukhantsev-Korneev, F Rossi *Surf. Coat. Technol.* **182** 101 (2004)
103. D V Shtansky, E A Levashov, N A Glushankova, I V Lyasotskii, F Rossi *Fiz. Met. Metalloved.* **97** 34 (2004) [d]
104. D V Shtansky, I A Bashkova, E A Levashov, T A Chipysheva, Yu M Vasil'ev, N A Glushankova *Dokl. Akad. Nauk* **404** 267 (2005) [e]
105. W Kulisch, P Colpo, P N Gibson, G Ceccone, D V Shtansky, E A Levashov, F Rossi *Surf. Coat. Technol.* **188 – 189** 735 (2004)
106. W Kulisch, P Colpo, F Rossi, D V Shtansky, E A Levashov *Surf. Coat. Technol.* **188 – 189** 714 (2004)
107. W Kulisch, P Colpo, P N Gibson, G Ceccone, D V Shtansky, E A Levashov, M Jelinek, P J M Philip, F Rossi *Appl. Phys. A: Mater. Sci. Process.* **82** 503 (2006)
108. J C Imbert, L de Poucques, C Boisse-Laporte, J Bretagne, M C Hugon, L Teulé-Gay, M Touzeau, D Shtansky, O Voldoire *Surf. Coat. Technol.* **200** 717 (2005)
109. A Leyland, A Matthews *Surf. Coat. Technol.* **177 – 178** 317 (2004)
110. K Anselme *Biomaterials* **21** 667 (2000)
111. C M Champagne, J Takebe, S Offenbacher, L F Cooper *Bone* **30** 26 (2002)
112. P L E M Van Lent, A B Blom, P Van der Kraan, A E M Holthuysen, E Vitters, N Van Rooijen, R L Smeets, K C A M Nabbe, W B Van den Berg *Arthritis Rheum.* **50** 103 (2004)
113. J M Wozney *Spine* **27** (16S) S2 (2002)

[a] — *Phys. Solid. State (Engl. Transl.)*
[b] — *Mendeleev Chem. J. (Engl. Transl.)*
[c] — *Dokl. Phys. (Engl. Transl.)*
[d] — *Phys. Met. Metallogr. (Engl. Transl.)*
[e] — *Dokl. Biochem. Biophys. (Engl. Transl.)*